Letters

Investigating the Current Collapse Mechanisms of p-GaN Gate HEMTs by Different Passivation Dielectrics

Xiangdong Li, *Member, IEEE*, Niels Posthuma, Benoit Bakeroot, Hu Liang, Shuzhen You, Zhicheng Wu, Ming Zhao, Guido Groeseneken, *Fellow, IEEE*, and Stefaan Decoutere

***Abstract*—In this letter, the dynamic R_{on} degradation mechanisms of the p-GaN gate HEMTs induced by OFF-state stress are investigated with different passivation dielectrics AlON and SiN. The degradation mechanisms are twofold, including V_{TH} shift and surface trapping in the gate-to-drain access region, whose impacts are successfully distinguished. Surface trapping by SiN passivation is evidently proved to be the dominant factor that can almost induce a full current collapse. The V_{TH} positive shift diminishes the drain current by shrinking the overdrive V_{GS}, which however, can be compensated by a higher V_{GS} overdrive in applications. SiN passivation can effectively suppress the positive bias temperature instability effect, probably by passivating the p-GaN fast traps with hydrogen during passivation. Last, the transient measurements unveil that both the surface trapping and V_{TH} shift have a very slow recovery process.**

***Index Terms*—Dynamic R_{ON}, p-GaN gate HEMTs, surface trapping, V_{TH} shift.**

I. Introduction

COMMERCIALIZATION of the enhancement-mode (e-mode) p-GaN gate HEMTs has been started recently, especially in the field of consumer electronics such as fast chargers [1]–[4]. There are mainly two types of e-mode HEMTs available, i.e., Schottky-type p-GaN gate HEMTs [1], [2] and hybrid-drain-embedded gate injection transistor [3], [4]. Reliability issues beyond the JEDEC standard [5] such as current collapse, p-GaN gate failure, V_{TH} shift, etc., have been hampering the wide applications of the GaN power electronic devices.

Manuscript received September 4, 2020; revised September 28, 2020; accepted October 13, 2020. Date of publication October 16, 2020; date of current version January 22, 2021. This work was supported in part by the Vlaams Agenschap Innoveren en Ondernemen and in part by the IMEC.ICON Research Program under Grant HBC.2017.0632. *(Corresponding author: Xiangdong Li.)*

Xiangdong Li, Zhicheng Wu, and Guido Groeseneken are with the Department of Electrical Engineering, KU Leuven, 3001 Leuven, Belgium, and also with the imec, 3001 Leuven, Belgium (e-mail: xiangdong.li@imec.be; zhicheng.wu@imec.be; guido.groeseneken@imec.be).

Niels Posthuma, Hu Liang, Shuzhen You, Ming Zhao, and Stefaan Decoutere are with the imec, 3001 Leuven, Belgium (e-mail: niels.posthuma@imec.be; hu.liang@imec.be; shuzhen.you@imec.be; ming.zhao@imec.be; stefaan.decoutere@imec.be).

Benoit Bakeroot is with the Center for Microsystems Technology, imec, Ghent University, 9052 Ghent, Belgium (e-mail: benoit.bakeroot@imec.be).

Color versions of one or more of the figures in this letter are available online at https://ieeexplore.ieee.org.

Digital Object Identifier 10.1109/TPEL.2020.3031680

Current collapse, or dynamic R_{ON} degradation, after high-voltage OFF-state stress has been heavily investigated for a long time. This problem is normally ascribed to several possible reasons including: 1) surface trapping in the gate-to-drain access region [6], [7]; 2) V_{TH} positive shift [8]– [11]; and 3) buffer trapping [12]–[14]. For the Schottky-type p-GaN gate HEMTs, we have previously demonstrated p-GaN gate HEMTs with the current collapse well limited within $\pm 20\%$ by a bi-layer passivation [15], [16]. It has also been unveiled that dedicated buffer stack design and surface passivation can effectively suppress the buffer trapping [14] and surface trapping [6].

Although the surface trapping and V_{TH} positive shift have been experimentally confirmed to contribute to the current collapse, their impacts are however difficult to be distinguished. Plus, the impact of passivation on the V_{TH} is seldom reported. In this work, the trapping and de-trapping behaviors will be unambiguously identified on the p-GaN gate HEMTs with different passivation dielectrics. Double-pulsed *I-V* and transient measurements will be conducted to stress and monitor the recovery behavior of the trapping effects. It is noticed that some works have evaluated the dynamic R_{on} by various specifically practical circuits [17], [18]. In contrast, we present some more fundamental findings that might not cover all the issues in real applications but is instructive for device design, understanding, and manufacturing.

II. Epitaxy and Fabrication

The p-GaN/AlGaN/GaN structure was epitaxially grown by a metalorganic chemical vapor deposition on 200 mm p^+-Si substrates. The epi stack comprises an AlN nucleation layer, a superlattice layer, a C:GaN layer, a GaN channel layer, an AlGaN barrier layer, and a Mg-doped p-GaN layer. Detailed processing can be found in [15]. The measured dc and power HEMTs have a gate width W_G of 100 μm and 36 mm, respectively. They share the same gate length L_G of 1.5 μm, gate-source distance L_{GS} of 0.75 μm, and gate-drain distance L_{GD} of 16 μm. There are four field plates with lengths of 2, 4, 6, and 8 μm, measured from the gate edge of the drain side. Two wafers were compared with different passivation dielectrics of AlON and SiN on top of the AlGaN barrier layer. The double-pulsed measurements were performed using an Auriga AU4850 pulsed

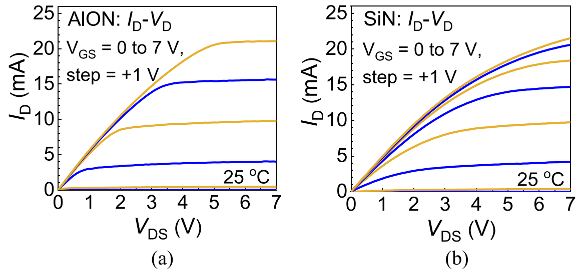

Fig. 1. Output characteristics of the 100 μm (a) AlON-passivated and (b) SiN-passivated HEMTs at 25 °C.

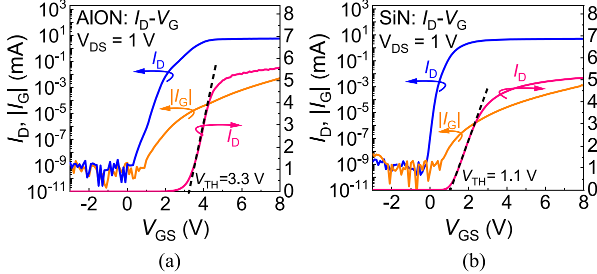

Fig. 2. Transfer characteristics of the 100 μm (a) AlON-passivated and (b) SiN-passivated HEMTs at 25 °C.

IV/RF characterization system. The dc and transient recovery measurements were performed by Keysight B1505A. The fast sweeping measurements were conducted by Keysight B1530A WGFMU (Waveform Generator/Fast Measurement Unit).

III. Results and Discussion

Figs. 1 and 2 show the I_D-V_D output characteristics and I_D-V_G transfer characteristics of the 100-μm dc HEMTs. The SiN-passivated HEMTs feature a low V_{TH} of 1.1 V and a very sharp subthreshold slope, implying the SiN passivation can significantly impact the electrical performance of the p-GaN gate HEMTs. AlON-passivated HEMTs resemble the previous reported devices with a high $V_{TH} > 3$ V and a smoother subthreshold slope, ascribed to the trapping effect in the p-GaN layer [19], [20].

Fast sweeping I_D-V_G curves by B1530A WGFMU are demonstrated in Fig. 3(a). Strikingly, the hysteresis of the SiN-passivated HEMTs is as small as 70 mV. Further positive bias temperature instability (PBTI) characterization was conducted by stressing the gate by 6 and 5 V on the AlON-passivated and SiN-passivated HEMTs, respectively. During the characterization, their source terminals were grounded, and the drain terminals were biased at 50 mV. It is shown in Fig. 3(b) that the SiN-passivated HEMTs possess a lower but much more stable V_{TH}. This behavior is probably induced by the hydrogen passivation effect, where the hydrogen is introduced during the SiN deposition. It is worthwhile to mention that only the fast characterization can observe such a significant hysteresis and V_{TH} instability effect on AlON-passivated HEMTs, because of the p-GaN fast trapping and de-trapping characteristics [19].

To characterize the current collapse, the devices were then subjected to double-pulsed I_D-V_D measurements. The

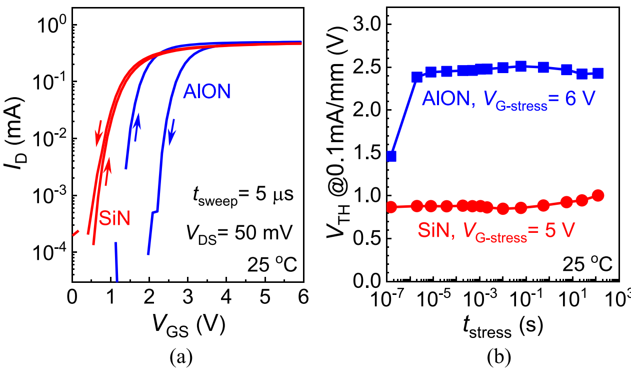

Fig. 3. (a) Double-sweep I_D-V_G curves and (b) V_{TH} evolution during the forward gate voltage stress of the 100-μm AlON-passivated and SiN-passivated HEMTs, by the fast sweeping measurements with an ultrashort I_D-V_G sweep time t_{sweep} of 5 μs.

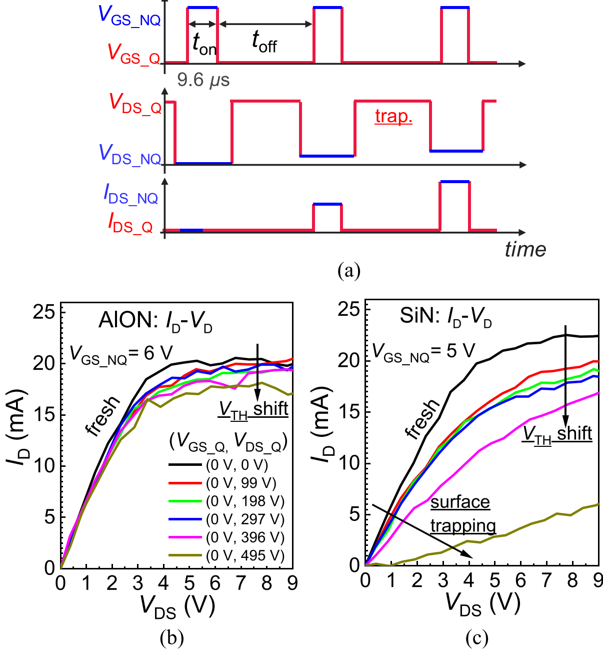

Fig. 4. Double-pulsed I_D-V_D (a) waveforms and I_D-V_D curves for the 100-μm (b) AlON-passivated HEMTs and (c) SiN-passivated HEMTs. The quiescent stressing $V_{DS\text{-}Q}$ is 0, 99, 198, 297, 396, and 495 V.

waveforms are depicted in Fig. 4(a). In the OFF state, the devices were stressed by ($V_{GS\text{-}Q}$, $V_{DS\text{-}Q}$) to induce the drain current collapse, followed by a short dead-time of 200 ns. Afterward, the devices were turned on by the ($V_{GS\text{-}NQ}$, $V_{DS\text{-}NQ}$), thus the drain current can be monitored after each OFF-state stress. The drain current sampling aperture is 5 μs to record the impact of the OFF-state stress. The t_{on} is 9.6 μs and the t_{off} is 1990 μs. This low duty cycle of 0.5% is to protect the pulse header from burning. It is known that the drain current decrease in the I_D-V_D saturation region and linear region is the signature of V_{TH} shift and trapping in the access region, respectively [21]. Fig. 4(b) and (c) clearly indicates that these two devices both suffer from V_{TH} shifts, because their drain currents in the saturation region see a reduction. However, only the SiN-passivated HEMTs show a significant current collapse in the I_D-V_D linear region, proving these devices possess a dramatic trapping in

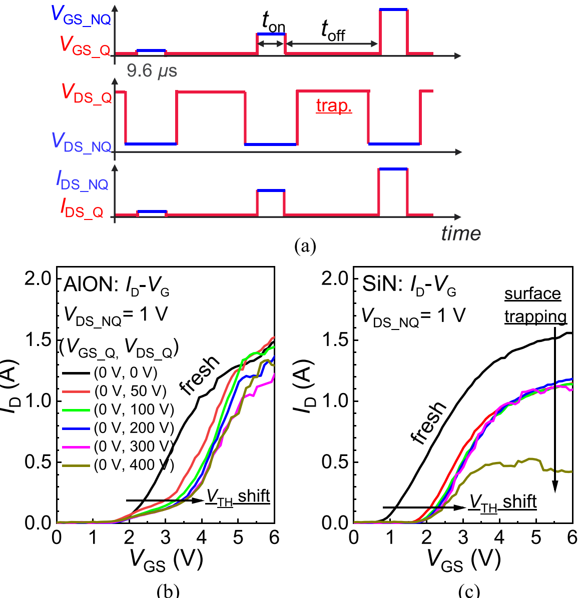

Fig. 5. Double-pulsed I_D-V_G (a) waveforms and I_D-V_G curves for the 36-mm (b) AlON-passivated HEMTs and (c) SiN-passivated HEMTs. The quiescent stressing $V_{DS\text{-}Q}$ is 0, 50, 100, 200, 300, and 400 V.

the gate-to-drain access region. Considering the two devices have the identical epitaxy and structure, passivation is therefore confirmed to directly induce this degradation. 100-μm small p-GaN gate HEMTs were measured in Fig. 4 because of the current compliance.

To further uncover the mechanisms responsible for the current collapse, double-pulsed I_D-V_G measurements were performed as shown in Fig. 5, which can quantitatively distinguish the impact by different factors. Both devices show a large V_{TH} shift of more than 1 V. The AlON-passivated HEMTs give an abnormal current bump in the voltage range from 2 to 4 V. This is similar to the results in [19] and [20], which are possibly induced by trapping under the gate.

Notably, the I_D of the AlON-passivated HEMTs at $V_{GS} = 5$ V under the stress condition of (0 V, 0 V) reaches 1.2 A. The drain current decreases by 30% for $V_{GS} = 5$ V under the stress condition of (0, 400 V). To compensate this current collapse, the V_{GS} can be increased to 5.4 V in this stress case. Therefore, a large enough V_{GS} overdrive can effectively compensate the V_{TH} shift in real applications, provided the HEMTs are free of surface trapping. The SiN-passivated HEMTs demonstrate a definite evidence of surface trapping, especially under the stress condition of (0, 400 V), where the drain current decreases by 65%. This is similar to the excessive current collapse reported in literature of the GIT HEMTs under high-voltage stress [22].

It has been shown in Fig. 3(b) that SiN passivation can efficiently suppress the PBTI effect. However, the V_{TH} shift appears again under the OFF-state drain stress. This proves that the OFF-stress-induced V_{TH} shift possesses a different mechanism from that of the gate PBTI. Previous studies have also pointed out that, instead of the p-GaN trapping effect, the trapping taking place in the AlGaN barrier [8] and GaN buffer [9], or p-GaN charging effect [10] are possibly responsible for the OFF-stress-induced V_{TH} shift.

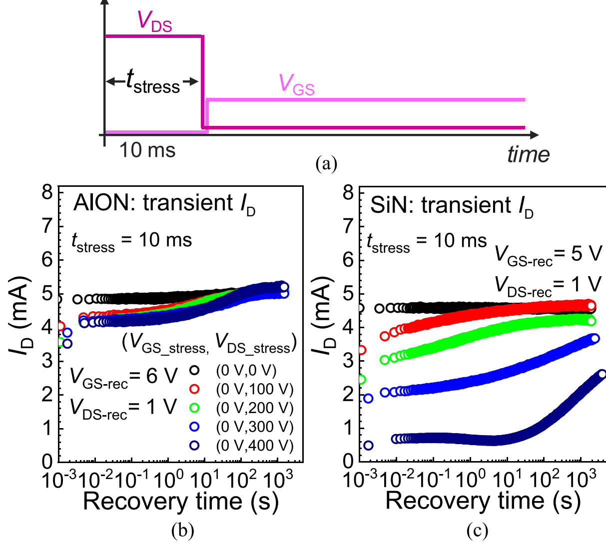

Fig. 6. (a) Stress and sense procedure, and the current transient waveforms of the 100-μm (b) AlON-passivated HEMTs and (c) SiN-passivated HEMTs during the recovery phase. The stress condition is $V_{GS} = 0$ V/ $V_{DS} = 400$ V and the stress time is 10 ms.

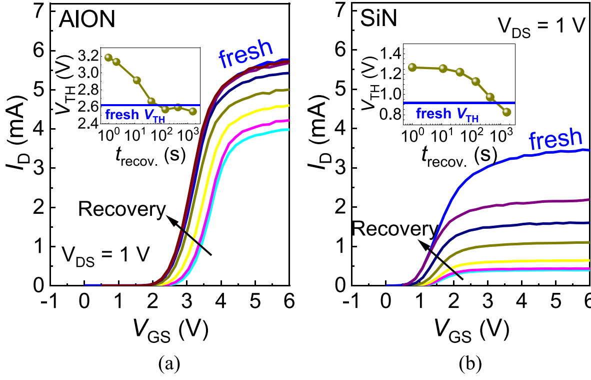

Fig. 7. Transfer I_D-V_G curves of the 100-μm (a) AlON-passivated HEMTs and (b) SiN-passivated HEMTs during the recovery phase. The stress condition is $V_{GS} = 0$ V/ $V_{DS} = 400$ V. The insets show the V_{TH} evolution during the recovery phase.

To monitor the de-trapping behavior, transient measurements were conducted with a Keysight B1505A. As shown in Fig. 6(a), the HEMTs were first subjected to a 10-ms OFF-state stress, then the stress was released, the HEMTs were switched ON and the drain current recovery behavior was recorded. There is around 3-ms transition time between the stress and recovery, which however, will not significantly jeopardize the monitoring. The AlON-passivated HEMTs show an almost constant current decrease of 13%, irrespective of the stressing voltages. In contrast, the SiN-passivated HEMTs show a monotonous current decrease with increasing stressing voltages.

The recovery process was periodically interrupted by the I_D-V_G sweeps as shown in Fig. 7. For the SiN-passivated HEMTs, the V_{TH} and surface trapping were recovering simultaneously. After 1490 s, the V_{TH} fully recovered, but the surface trapping still existed. For the AlON-passivated HEMTs, the V_{TH} recovery dominated the current recovery process. Due to the limitation of the setup, the transition between the recovery and sweep

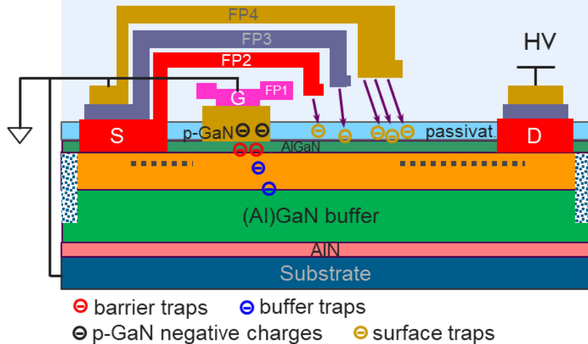

Fig. 8. Schematic cross section of the p-GaN gate HEMTs with four field plates. Possible trapping occurs in the AlGaN barrier, GaN buffer, and gate-to-drain access region, and negative charging of the p-GaN is depicted as well.

takes around 1 s, whose impact is visible, noticing the $V_{\rm TH}$ shift observed in Fig. 7 is less than 1 V compared with Fig. 5, because of some recovery already happened during this delay. However, the $V_{\rm TH}$ recovery and de-trapping processes are still quite clear because of the slow recovery behavior.

Based on the experiments and comparison above, the possible current collapse mechanisms are depicted in Fig. 8. The surface trapping in the gate-to-drain access region is evidently dominant if the passivation quality is imperfect, which can be efficiently suppressed by using the AlON passivation dielectric, or similarly with Al_2O_3 in our previous work [15]. Another dominant factor of $V_{\rm TH}$ shift possibly stems from the trapping effects in the AlGaN barrier and GaN buffer, or from the p-GaN charging effect due to the charged gate-to-drain capacitance $C_{\rm GD}$. The $V_{\rm TH}$ shifts induced by the OFF-state drain-voltage stress and ON-state gate-voltage stress seem different from each other, because the OFF-stress-induced $V_{\rm TH}$ shift has a recovery time constant of around 10 to 100 s (see Fig. 7), whereas the PBTI effect time constant is approximately 1 ms [19].

IV. Conclusion

Current collapse caused by $V_{\rm TH}$ shift and trapping in the gate-to-drain access region has been successfully distinguished and confirmed by passivating the p-GaN gate HEMTs with different dielectrics AlON and SiN. The trapping and de-trapping behaviors were comprehensively monitored by various characterization methods such as fast sweeping, double-pulsed $I_{\rm D}$-$V_{\rm D}$ and $I_{\rm D}$-$V_{\rm G}$, and transient measurements. The $V_{\rm TH}$ shift by OFF-state stress was found to always exist in the Schottky-type p-GaN gate HEMTs, which, however, can be compensated by a large gate overdrive voltage. The trapping in the access region that induces a severe current collapse was proved to exactly locate in the SiN dielectric. This trapping can induce an almost full current collapse at high OFF-state $V_{\rm DS}$ of 400 V, which can be effectively suppressed by using the high-quality AlON or Al_2O_3 passivation layer. Both the $V_{\rm TH}$ recovery and surface de-trapping processes are very slow. Moreover, SiN passivation was found to be able to efficiently suppress the PBTI effect, probably by passivating the p-GaN fast traps with hydrogen.

Acknowledgment

The authors would like to thank ASM for the contribution on the AlON dielectric layer deposition.

References

[1] Navitas, NV6115 Datasheet. 2018. [Online]. Available: https://www.navitassemi.com
[2] GaNSystem, GS66504B Datasheet. 2018. [Online]. Available: https://gansystems.com
[3] Infineon, IGT60R190D1S Datasheet. 2020. [Online]. Available: https://www.infineon.com
[4] Panasonic, PGA26E07BA, Datasheet. 2019. [Online]. Available: https://industrial.panasonic.com
[5] Wide Bandgap Power Semiconductors: GaN, SiC. 2020. [Online]. Available: https://www.jedec.org/category/technology-focus-area/wide-bandgap-power-semiconductors-gan-sic
[6] M. Meneghini *et al.*, "Temperature-dependent dynamic $R_{\rm ON}$ in GaN-based MIS-HEMTs: Role of surface traps and buffer leakage," *IEEE Trans. Electron. Devices*, vol. 62, no. 3, pp. 782–787, Mar. 2015.
[7] R. Vetury, N. Q. Zhang, S. Keller, and U. K. Mishra, "The impact of surface states on the DC and RF characteristics of AlGaN/GaN HFETs," *IEEE Trans. Electron. Devices*, vol. 48, no. 3, pp. 560–566, Mar. 2001.
[8] L. Efthymiou, K. Murukesan, G. Longobardi, F. Udrea, A. Shibib, and K. Terrill, "Understanding the threshold voltage instability during OFF-state stress in p-GaN HEMTs," *IEEE Electron. Device Lett.*, vol. 40, no. 8, pp. 1253–1256, Aug. 2019.
[9] J. Chen *et al.*, "OFF-state drain-voltage-stress-induced $V_{\rm TH}$ instability in Schottky-type p-GaN gate HEMTs," *IEEE J. Emerg. Sel. Top. Power Electron.*, to be published, doi: 10.1109/JESTPE.2020.3010408.
[10] J. Wei *et al.*, "Charge storage mechanism of drain induced dynamic threshold voltage shift in p-GaN gate HEMTs," *IEEE Electron. Device Lett.*, vol. 40, no. 4, pp. 526–529, Apr. 2019.
[11] S. Yang, S. Han, K. Sheng, and K. J. Chen, "Dynamic on-resistance in GaN power devices: Mechanisms, characterizations, and modeling," *IEEE J. Emerg. Sel. Topics Power Electron.*, vol. 7, no. 3, pp. 1425–1439, Sep. 2019.
[12] M. J. Uren *et al.*, "'Leaky dielectric' model for the suppression of dynamic $R_{\rm ON}$ in carbon-doped AlGaN/GaN HEMTs," *IEEE Trans. Electron. Devices*, vol. 64, no. 7, pp. 2826–2834, Jul. 2017.
[13] S. Yang, C. Zhou, S. Han, J. Wei, K. Sheng, and K. J. Chen, "Impact of substrate bias polarity on buffer-related current collapse in AlGaN/GaN-on-Si power devices," *IEEE Trans. Electron. Devices*, vol. 64, no. 12, pp. 5048–5056, Dec. 2017.
[14] S. Stoffels *et al.*, "The physical mechanism of dispersion caused by AlGaN/GaN buffers on Si and optimization for low dispersion," in *Proc. IEEE Int. Electron. Devices Meeting*, Dec. 2015, pp. 35.4.1–35.4.4.
[15] N. E. Posthuma, S. You, S. Stoffels, H. Liang, M. Zhao, and S. Decoutere, "Gate architecture design for enhancement mode p-GaN gate HEMTs for 200 and 650 V applications," in *Proc. IEEE 30th Int. Symp. Power Semicond. Devices ICs*, May 2018, pp. 188–191.
[16] X. Li *et al.*, "GaN-on-SOI: Monolithically integrated All-GaN ICs for power conversion," in *Proc. IEEE Int. Electron. Devices Meeting*, 2019, pp. 4.4.1–4.4.4.
[17] G. Zulauf, M. Guacci, and J. W. Kolar, "Dynamic on-resistance in GaN-on-Si HEMTs: Origins, dependencies, and future characterization frameworks," *IEEE Trans. Power Electron.*, vol. 35, no. 6, pp. 5581–5588, Jun. 2020.
[18] P. J. Martínez, P. F. Miaja, E. Maset, and J. Rodríguez, "A test circuit for GaN HEMTs dynamic $R_{\rm ON}$ characterization in power electronics applications," *IEEE J. Emerg. Sel. Topics Power Electron.*, vol. 7, no. 3, pp. 1456–1464, Sep. 2019.
[19] X. Li *et al.*, "Observation of dynamic $V_{\rm TH}$ of p-GaN gate HEMTs by fast sweeping characterization," *IEEE Electron. Device Lett.*, vol. 41, no. 4, pp. 577–580, Apr. 2020.
[20] O. Hilt, A. Knauer, F. Brunner, E. Bahat-Treidel, and J. Wurfl, "Normally-off AlGaN/GaN HFET with p-type GaN gate and AlGaN buffer," in *Proc. 6th Int. Conf. Integr. Power Electron. Syst.*, 2010, pp. 1–4.
[21] D. Bisi *et al.*, "Trapping mechanisms in GaN-based MIS-HEMTs grown on silicon substrate," *Phys. Status Solidi A*, vol. 212, no. 5, pp. 1122–1129, May 2015.
[22] K. Tanaka *et al.*, "Suppression of current collapse by hole injection from drain in a normally-off GaN-based hybrid-drain-embedded gate injection transistor," *Appl. Phys. Lett.*, vol. 107, no. 10, Oct. 2015, Art. no. 163502.